CLIMATOLOGY

10.1126/sciadv.1500806

Glacier maxima in Baffin Bay during the Medieval Warm Period coeval with Norse settlement

Nicolás E. Young,[1]* Avriel D. Schweinsberg,[2] Jason P. Briner,[2] Joerg M. Schaefer[1,3]

The climatic mechanisms driving the shift from the Medieval Warm Period (MWP) to the Little Ice Age (LIA) in the North Atlantic region are debated. We use cosmogenic beryllium-10 dating to develop a moraine chronology with century-scale resolution over the last millennium and show that alpine glaciers in Baffin Island and western Greenland were at or near their maximum LIA configurations during the proposed general timing of the MWP. Complimentary paleoclimate proxy data suggest that the western North Atlantic region remained cool, whereas the eastern North Atlantic region was comparatively warmer during the MWP—a dipole pattern compatible with a persistent positive phase of the North Atlantic Oscillation. These results demonstrate that over the last millennium, glaciers approached their eventual LIA maxima before what is considered the classic LIA in the Northern Hemisphere. Furthermore, a relatively cool western North Atlantic region during the MWP has implications for understanding Norse migration patterns during the MWP. Our results, paired with other regional climate records, point to nonclimatic factors as contributing to the Norse exodus from the western North Atlantic region.

INTRODUCTION

Following early Holocene warmth, millennial-scale cooling through the Holocene Epoch (the past 11,700 years) in the Northern Hemisphere has been superposed by centennial-scale climate change, culminating in the transition from the Medieval Warm Period (MWP; ~950 to 1250 CE) (*1*) to the Little Ice Age (LIA; ~1300 to 1850 CE) (*2*). Although the Holocene's long-term cooling trend is presumably driven by a gradual reduction in summer insolation, the proposed driving mechanisms of centennial-scale variability remain under debate, but possible mechanisms include variations in solar irradiance (*3*), the strength of the Atlantic meridional overturning circulation (*4*), volcanism coupled with sea ice/ocean–related feedbacks (*5*), and internal modes of atmospheric variability (*6*, *7*). The perceived warmth of the MWP, with a North Atlantic climate favorable for sea voyage and increased crop yield, has often been invoked as a catalyst for Norse migration into the western North Atlantic region (*8*, *9*). The Norse settled in Greenland in ~985 CE (*10*) and expanded to establish temporary settlements on northern Newfoundland, and possibly on southern Baffin Island, by ~1000 CE (*11*–*13*). The Norse remained in Greenland for almost four centuries before abandoning the Western and Eastern Settlements in Greenland at ~1360 and ~1450 CE, respectively (*14*). Reasons behind initial Norse settlement and eventual demise remain controversial; some suggest that mild conditions and decreased sea ice during the MWP, followed by deteriorating climate during the LIA, were the primary factors influencing Norse migration patterns (*14*, *15*), whereas others note Norse resilience and suggest that alternative socioeconomic factors, such as a decrease in Norse shipping and trading opportunities, led to the Norse leaving their Greenland settlements (*16*, *17*). Developing robust regional records of climate variability that span the MWP-LIA interval can help determine which climatic mechanisms drive regional centennial- to subcentennial-scale climate variability, and can provide a fundamental framework to evaluate Norse cultural adaptations to key climate system changes.

[1]Lamont-Doherty Earth Observatory of Columbia University, Palisades, NY 10964, USA. [2]Department of Geology, University at Buffalo, Buffalo, NY 14260, USA. [3]Department of Earth and Environmental Sciences, Columbia University, NY 10027, USA.
*Corresponding author. E-mail: nicolasy@ldeo.columbia.edu

Glaciers are highly sensitive to changes in temperature and precipitation (*18*), and accordingly, past fluctuations in glacier extent can be used to robustly reconstruct past changes in climate. Where glacier termini intersect tree line, precise glacier histories that span millennia can be reconstructed (*19*), but unfortunately, Arctic glaciers have not intersected tree line during the late Holocene. Hence, reconstructing Arctic glacier change has proven difficult. Moraines deposited on the landscape mark former glacier dimensions; these markers, in conjunction with knowledge of the timing of their deposition, can be used to reconstruct glacier histories and extract key climate information (*20*–*22*). Most alpine glaciers in the Northern Hemisphere reached their maximum Holocene extent sometime during the LIA, consistent with the long-term reduction in Northern Hemisphere insolation (*23*). Thus, only moraines dating to the LIA or younger are typically preserved on the landscape, and consequently, directly dating these preserved moraines results in glacier histories that only span the past few hundred years. However, in some unique settings, moraines that were deposited before the LIA are preserved and present an opportunity to develop longer glacier reconstructions. Initial attempts to directly date LIA and pre-LIA moraines in the Arctic relied on lichenometry (*24*), but large chronological uncertainties prevent establishing centennial-scale records of glacier change (*25*). Here, we exploit glacial geomorphic settings in Baffin Island and western Greenland, where rare late Holocene moraine sequences document glacier configuration before the last few hundred years. We date these moraines with cosmogenic ^{10}Be, capitalizing on a high-precision local ^{10}Be production rate (*26*) and high measurement precision for low-level ^{10}Be concentrations to establish a record of glacier change in the western North Atlantic region over the last millennium with centennial-scale resolution.

RESULTS

Moraine preservation

We targeted moraine systems in Naqsaq and in Ayr Lake valleys, Baffin Island (Figs. 1 and 2), and we focused on a moraine system in the Uigordleq Lake valley, western Greenland (Fig. 1 and fig. S1; see

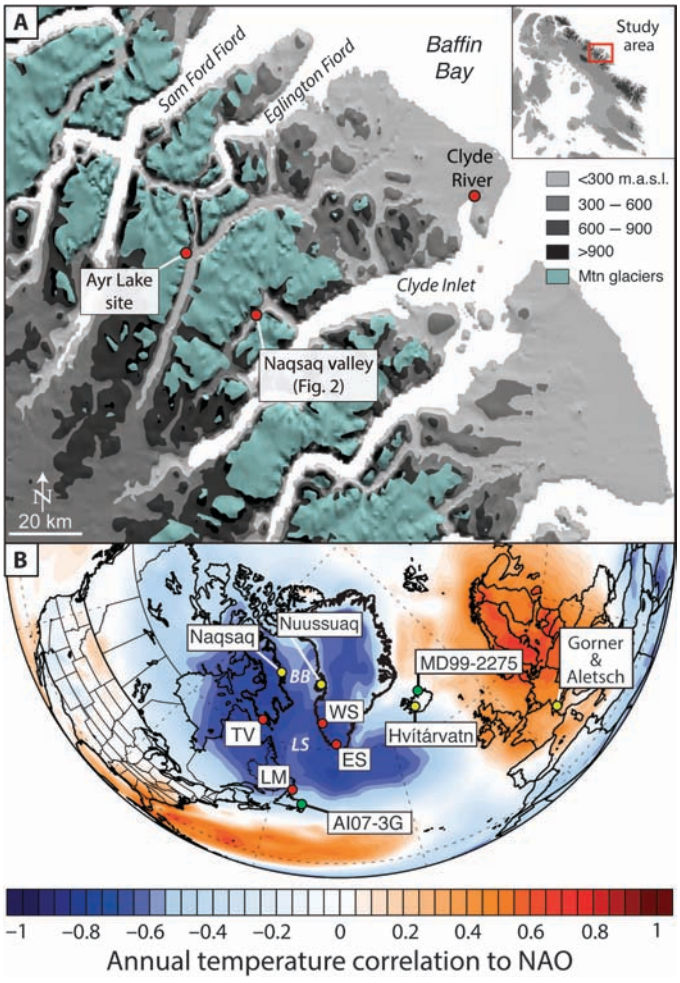

Fig. 1. Baffin Island and the North Atlantic region. (**A**) Study region in Baffin Island. (**B**) North Atlantic region with annual temperature correlation to the North Atlantic Oscillation (NAO) based on the European Reanalysis Interim data set, 1979–2013 (principal component–based; image obtained using U. Maine Climate Reanalyzer, www.cci-reanalyzer.org). Shown are the locations of the Naqsaq valley and Nuussuaq Peninsula study areas, alkenone-based sea surface temperature (SST) records from MD99-2275 and AI07-2G (*35*), proglacial lake sediment record from Hvítárvatn, and the location of the Gorner and Aletsch glaciers. Locations of Norse settlements (red dots): Eastern Settlement (ES), Western Settlement (WS), L'Anse aux Meadows (LM), and Tanfield valley (TV), a possible Norse site (*12*, *13*). BB, Baffin Bay; LS, Labrador Sea.

Materials and Methods). The preservation of several late Holocene moraines in the Naqsaq valley is likely a function of local topography. The terminus of the Naqsaq glacier spills onto the main trunk valley floor that slopes to the northeast (NE). Thus, once the Naqsaq glacier advances far enough to intersect the main valley floor, the glacier is predisposed to follow the valley gradient and flow to the NE, resulting in the preservation of pre-LIA moraines on the southwest (uphill) side of the valley (Fig. 2; main text). Supporting this concept is the observation that no pre-LIA moraines are preserved on the NE (downhill) side of the glacier—the left-lateral moraine equivalents of our preserved right-lateral moraines have been overrun by successive LIA glacier advances. Similarly, the preserved right-lateral moraines in Ayr and Uigordleq Lake valleys are found on the uphill side of the main Ayr Lake valley and Uigordleq sarqâ, respectively.

^{10}Be ages

We sampled 20 boulders in Naqsaq valley, 4 boulders in Ayr Lake valley, and 9 boulders in Uigordleq Lake valley (Fig. 2, fig. S1, tables S1 and S2). All ^{10}Be ages were calculated using the locally calibrated Baffin Bay production rate (*26*) and time-variant "Lm" scaling; however, because our study sites rest at such high latitude (~70°N), ^{10}Be ages vary by only ~2% with alternate scaling schemes (table S3). Indeed, the effects of geomagnetic field fluctuations on ^{10}Be production are minimal at this high latitude (see Materials and Methods). In addition, we made no correction for potential snow cover, surface erosion, isostatic uplift, or moraine degradation, but we point readers to Materials and Methods for a fuller discussion of these variables (see Geologic and geomorphic setting, and ^{10}Be production rate, ^{10}Be age calculations, and ^{10}Be assumptions). Individual ^{10}Be ages are presented with their 1σ analytical uncertainties, which include the uncertainty in the blank correction; ages are then rounded to the nearest decade. When assigning moraine ages that are compared to independently dated records of climate variability, we take the arithmetic mean and standard deviation (SD) of each ^{10}Be age population and then propagate through in the quadrature the uncertainty in the Baffin Bay ^{10}Be production rate. The Baffin Bay ^{10}Be production rate comprises three independent and statistically indistinguishable calibration data sets that span the last ~8200 to 9200 years: two from Disko Bugt in western Greenland and one from Clyde Inlet, Baffin Island. Combined, these independent data sets result in a regional production rate with 1.8% uncertainty. A recent effort to characterize all sources of uncertainty has suggested a total systematic uncertainty of ~8 to 11% for ^{10}Be-based measurement populations (*27*). We acknowledge this estimate but report our ages as the arithmetic mean ± SD, with the production rate uncertainty propagated through because this approach is most commonly used in the literature. Adopting a systematic ~8 to 11% uncertainty for our moraine ages would only affect their accuracy and not their precision, and thus would not affect our ability to resolve differences in moraine age, nor would it affect our interpretations and conclusions.

Twenty ^{10}Be ages from the Naqsaq valley moraine sequence range from 6920 ± 140 years to 240 ± 20 years (±1σ analytical uncertainties; Fig. 2). Sample ELB-05 resting on the M4 crest has a ^{10}Be age of 6920 ± 140 years and likely contains ^{10}Be inherited from a previous period of exposure because it is ~5700 years older than any other ^{10}Be age, including ^{10}Be ages on stratigraphically older moraines (Fig. 2 and table S1), and it is >3σ older than the remaining M4 ages; we exclude this sample from further discussion. After removal of this single outlier, the remaining ages are internally self-consistent and the arithmetic mean of ^{10}Be ages for our five dated moraines in Naqsaq valley (±1σ; expressed as year CE with the production rate uncertainty propagated through) are 1040 ± 60 CE (n = 5), 1070 ± 100 CE (n = 3), 1220 ± 30 CE (n = 5), 1570 ± 20 CE (n = 3; one outlier removed), and 1700 ± 80 CE (n = 3). These moraine ages are consistent with their stratigraphic order, thereby increasing our confidence in the precision of the moraine ages (Fig. 2).

To further characterize our data set, we calculated the reduced χ^2 values of our ^{10}Be age populations on each moraine. A reduced χ^2 value of >1 suggests that the variance of ^{10}Be ages on a moraine is greater than what is attributable to measurement uncertainty alone, and thus, it is likely that geomorphic processes are contributing to

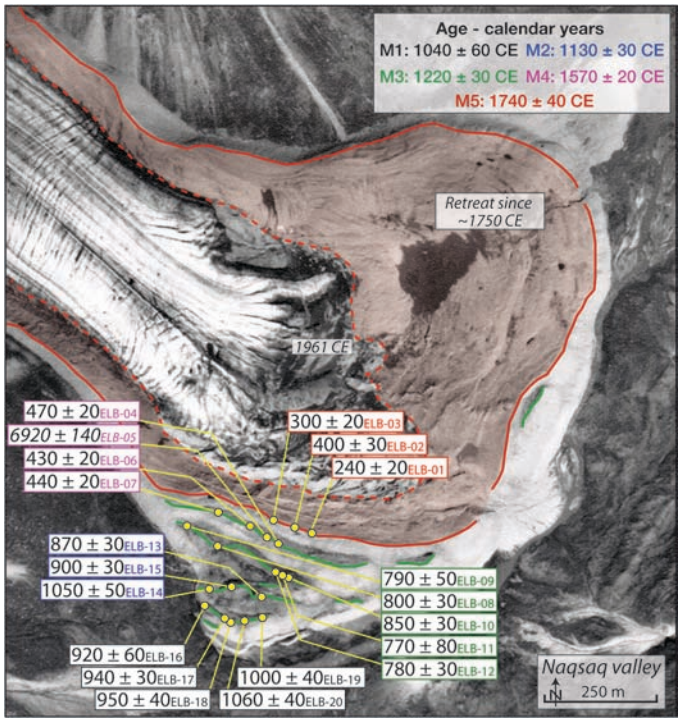

Fig. 2. Naqsaq valley ^{10}Be ages. Moraine ages are consistent with their stratigraphic order. Base image is a 1961 CE aerial photograph.

the variance (*28*). The reduced χ^2 values for M1 to M5 are 1.98, 6.76, 0.83, 0.54, and 14.20. These values suggest that M2 and M5 may have ^{10}Be ages that are affected by geomorphic processes. Previous authors have rejected outlying samples based on their contribution to the reduced χ^2 value and reject samples until the value is close to 1 [for example, Stroup *et al.* (*22*) and Putnam *et al.* (*29*)]. Adopting this same approach, we reject only two samples. Moreover, after considering the classic rules of morphostratigraphy, we suspect that these two samples are recycled boulders. Sample ELB-14 (1050 ± 50 years) resting on the M2 crest is considerably older than M2 samples ELB-13 and ELB-15 that have ages of 870 ± 30 and 900 ± 30 years, but is consistent with the ^{10}Be ages on M1, a stratigraphically older moraine (ranging from 920 ± 60 years to 1060 ± 40 years). Thus, it is possible that ELB-14 was first deposited on the landscape following ice retreat from M1, and then subsequently reincorporated into the glacier and deposited on M2 at the culmination of a glacier readvance. In a similar fashion, the ^{10}Be age of 400 ± 30 years (ELB-02) on M5 is consistent with the ^{10}Be ages on M4 (ranging from 430 ± 20 years to 470 ± 20 years). Again, it is possible that ELB-02 was initially deposited on the landscape during deglaciation from M4 and then reincorporated into the glacier and deposited on M5 at the culmination of a glacier readvance. After excluding samples ELB-14 and ELB-02, the reduced χ^2 values for M2 and M5 drop considerably to 0.59 and 5.32, and the recalculated ages of M2 and M5 are 1130 ± 30 CE and 1740 ± 40 CE, respectively. Regardless of whether samples ELB-14 and ELB-02 are excluded, our calculated moraine ages are consistent with their stratigraphic order; however, we suggest that excluding these samples on the basis of their morphostratigraphic relationships and their contribution to each moraine's reduced χ^2 value results in more geologically valid M2 and M5 ages.

In Ayr Lake valley, we dated the outermost moraine crest of a similar moraine system to CE 1200 ± 20 (Fig. 1 and fig. S2; n = 3; one outlier removed; reduced χ^2 = 0.05), but we recognize that our stated uncertainty (±20 years) is likely artificially low because of our small sample size. We consider the ^{10}Be age of 1510 ± 40 years (AYR-02) an outlier. This age is >3σ older than the remaining ^{10}Be ages and likely contains ^{10}Be inherited from a previous period of exposure. In western Greenland, the innermost moraine is dated to 1130 ± 40 CE (n = 3; reduced χ^2 = 0.48), with at least two glacier advances occurring slightly before ~1130 CE (see Materials and Methods).

Combined, ^{10}Be ages from Baffin Island and western Greenland spanning the last ~1 thousand years mark some of the youngest ^{10}Be ages published to date. Comparable and even younger ^{10}Be ages have been published from high-elevation montane landscapes (*20*, *22*, *30*); however, samples presented from here rest near sea level (~95 to 360 m above sea level; table S1) where in situ ^{10}Be production is significantly lower than at higher elevations, resulting in typical sample ^{10}Be concentrations ranging from ~6000 to 1250 atoms g^{-1} (table S2). Despite these low concentrations, our Naqsaq valley samples achieved 1σ analytical errors ranging from 2.7 to 10.8%, with a mean of 4.7%, resulting in ^{10}Be ages for each moraine that are consistent with their stratigraphic order (Fig. 2 and table S1). Collectively, these moraine ages constitute the first ^{10}Be-based glacier chronology with century-scale resolution in the Arctic.

DISCUSSION

Because moraine preservation in our study areas is controlled by local topography, combined with the observation that most glacier forefields in the region typically only host fresh and unvegetated moraines, we consider our pre-LIA moraines to mark the timing of when glacier size was similar to, but not larger than, the ensuing LIA glacier size. These older Naqsaq valley moraines simply provide a snapshot of when regional glaciers were similar in size to those dating from the LIA; pre-LIA moraines likely existed in other regional glacier forefields, but the subsequent LIA advance destroyed these moraines in valleys where moraine preservation is not influenced by local topography. In addition, because of the destructive nature of glacier advances and their capacity to overrun previously deposited moraines, we consider the number of dated moraines in the Naqsaq valley to represent a minimum number of glacier culminations. This concept is classically illustrated by Gibbons *et al.* (*31*), who demonstrated that given a series of glacier advances of similar magnitudes within a single valley, it is unlikely that each associated moraine will be preserved on the landscape. In a similar fashion, the full Naqsaq moraine sequence is not found in the Ayr or Uigordleq Lake valleys. However, the moraine dated to 1220 ± 30 CE in the Naqsaq sequence is consistent, within uncertainties, to the moraine dated to 1200 ± 20 CE in the Ayr Lake valley. We suspect that these indistinguishable moraine ages represent the synchronous culmination of glacier advances in each valley in response to the same regional climate forcing, and that the Naqsaq glacier chronology represents a regional signal. Moreover, the moraine dated to 1130 ± 40 CE in the Uigordleq valley on the Nuussuaq Peninsula is consistent, within uncertainties, to the moraine dated to 1130 ± 30 CE in Naqsaq valley. It is possible that there were additional glacier advances and moraine building events not captured in the more complete Naqsaq valley record, but the time elapsed between

our dated moraines ranges from only ~90 to 350 years (Fig. 2 and fig. S2), leaving little time for additional glacier advances not captured in our chronology. Finally, it is possible that glaciers experienced different responses to the same regional climate forcing, resulting in asynchronous ^{10}Be-dated moraine chronologies [for example, Pratt-Sitaula *et al.* (*32*)]. However, our moraine chronologies are not necessarily asynchronous; rather, each glacier forefield has varying degrees of moraine preservation, and what moraines are preserved are chronologically consistent with each other.

The primary driver of glacier change in the Baffin Bay region is summer (ablation season) temperature, which currently accounts for ~90% of variations in interannual mass balance (*5*, *33*), and thus, we consider our late Holocene glacier record to primarily reflect changes in summer temperature. We cannot definitively rule out that significant changes in precipitation helped drive glacier advances recorded here, but records from Summit Greenland reveal that regional accumulation rates varied by only ~6% over the last 1200 years (*34*). As expected, the inner moraines in Naqsaq valley, dating to 1570 ± 20 CE and 1740 ± 40 CE, confirm that an extensive advance of mountain glaciers in the Baffin Bay region culminated within the classic LIA interval (Fig. 2). However, our ^{10}Be ages also reveal that alpine glaciers approached their eventual LIA maximum extents before the LIA between ~1000 and 1250 CE (Fig. 2 and fig. S2). The most remarkable feature of our glacier chronology is that glaciers were near their LIA maximum through the MWP between ~975 and 1275 CE (Fig. 3).

Additional proxy records from the broader western North Atlantic region corroborate cool temperatures through the MWP as suggested by our glacier record. A recent alkenone-based SST reconstruction that tracks the southern extent of the Labrador Current emanating out of Baffin Bay and the Labrador Sea depicts a sharp temperature drop at ~1000 CE with sustained cool conditions through ~1350 CE (Fig. 3F) (*35*). Moreover, a variety of marine proxy records point to cooler conditions and extensive coastal sea ice cover along western Greenland through the MWP (*36*). At Summit Greenland, δ^{15}N-δ^{40}Ar gas-derived temperatures from the GISP2 ice core are variable but depict cooling episodes at ~1000 to 1075 CE and ~1200 to 1400 CE (Fig. 3D) (*37*). Finally, an alkenone-based record of lake water temperature in western Greenland shows a significant warm peak ~1100 CE, followed immediately by the coldest temperatures of the last millennium between ~1140 and 1220 CE (Fig. 3D) (*38*). Overall, beyond the high-frequency complexity, we interpret these independent proxy records to support our glacier signal, indicating regional cool conditions through the MWP, perhaps interrupted by brief warming episodes. Our glacier record does not rule out periods of decadal warming between ~975 and 1275 CE, but the down-valley persistence of glaciers through this interval indicates that any warming was not of sufficient magnitude or duration to have driven glaciers significantly up-valley.

In contrast to proxy records from the western North Atlantic region, records from the eastern North Atlantic region generally support warm conditions during the MWP. Historical observations and paleo-data indicate that sea ice off the Iceland coast was not common during the MWP (*39*), and an SST reconstruction off northern Iceland depicts a sharp rise in temperatures beginning ~1000 through ~1350 CE (Fig. 3H) (*35*). Moreover, glaciers in Europe (*19*) and Iceland (*40*) were restricted during the MWP (Fig. 3, I and J). Combined, these regional proxy records pose a critical question: What mechanism can explain a climatic dipole across the North Atlantic during the

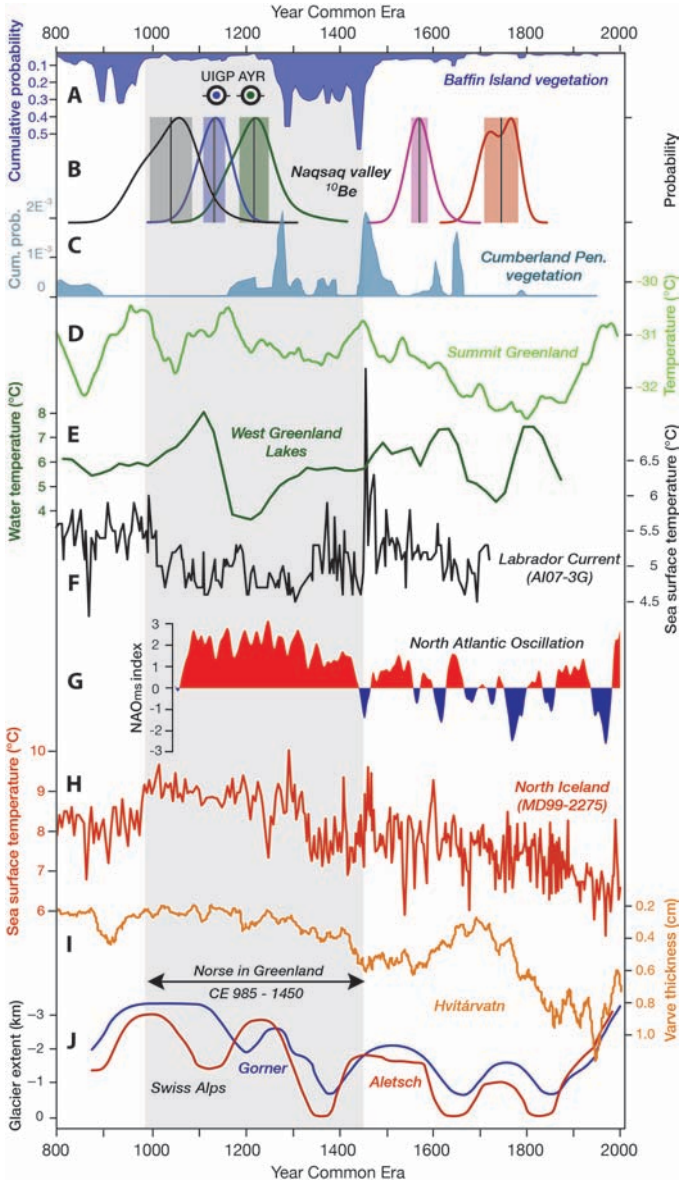

Fig. 3. Climate records across the North Atlantic region. (**A**) Summed probability of radiocarbon ages from Baffin Island marking the last period of plant growth and the onset of regional snowline lowering (*5*). (**B**) Summed probability of ^{10}Be ages from each moraine in the Naqsaq valley with the mean age and SD (fig. S2). Also shown are the dated moraines in Ayr Lake (AYR) and the proximal moraine in Uigordleq Lake valley (UIGP). (**C**) Summed probability of radiocarbon ages from the Cumberland Peninsula on southern Baffin Island (*64*). (**D**) Summit Greenland δ^{15}N-δ^{40}Ar gas-derived temperatures (*37*). (**E**) Alkenone-based lake temperatures in western Greenland (*38*). (**F**) Alkenone-based SSTs of the Labrador Current (*35*). (**G**) Reconstructed NAO index (*6*). (**H**) Alkenone-based SSTs off northern Iceland (*35*). (**I**) Varve thickness record from proglacial lake Hvítárvatn, Iceland (*40*). Increasing varve thickness represents increasing glacier size. (**J**) Glacier extent in the Swiss Alps (*19*).

MWP? A persistent positive state of the NAO, which has been cited as a driving mechanism behind the MWP in Europe (*6*) (Fig. 3G), would result in cooler conditions in the western North Atlantic region, including during the spring and autumn seasons along western Greenland which affect the magnitude of glacier ablation as recorded by modern and historical data (Fig. 1) (*41*). Indeed, the glacier and climate proxy data compiled here for the MWP are strikingly consistent with the climatic dipole pattern across the broader North Atlantic region during a sustained positive phase of the NAO [for example, Trouet *et al.* (*6*) and Sicre *et al.* (*35*)]. Within this framework, moraines deposited in Baffin Bay over the last millennium likely represent an interval when glaciers were situated down-valley, forced by the weakest insolation of the Holocene (that is, baseline glacier extent), whereas moraines deposited between ~1050 and 1220 CE include a response of mountain glaciers to a persistent NAO^+ state superposed on the long-term trend in insolation.

A persistent positive state of the NAO during the MWP has potentially important implications for understanding Norse migration patterns during the MWP-LIA interval. Norse migration from Iceland at 985 CE may have been facilitated in part by a favorable regional climate reigning in the eastern North Atlantic region, but the western North Atlantic region would have been characterized by extended glaciers and relatively cool climate during a positive NAO as depicted by several regional climate proxy records (Fig. 3). Thus, establishment and maturation of Norse society in Greenland occurred through a climate that was similar to that of the ensuing LIA, including the significant cooling episode ~1000 to 1075 CE that occurred almost immediately after initial settlement (Fig. 3). Moreover, significant LIA cooling did not occur until ~1600 CE, about 150 years after the Norse had left Greenland (Fig. 3), and it appears that the Norse occupied their Greenland settlements for several hundred years during a regionally cool MWP, perhaps interrupted by brief warming episodes. On the other hand, a cool western North Atlantic region during the summer does not necessarily indicate that the regional wintertime sea ice was anomalously extended. Indeed, Norse migration was highly dependent on regional sea ice extent, and restricted wintertime sea ice may still have allowed the Norse to migrate with relative ease. Regardless, the summertime climate records presented here point to regionally cool summers coinciding with Norse occupation, which, in turn, suggest that nonclimatic factors may have played an important role in driving Norse abandonment of the region. Devaluation of walrus tusks, the related Norse isolation via the stoppage of regular ship traffic from Norway and Iceland, and increasing hostilities with local Inuit were all possible factors that helped terminate the Norse presence in the western North Atlantic region (*16*, *17*). In any case, a ^{10}Be-dated moraine record with centennial-scale resolution reveals that glaciers in the western North Atlantic region were extended during the MWP and approached their eventual LIA maxima well before what is typically considered the classic Northern Hemisphere LIA, potentially linked to a sustained positive phase of the NAO.

MATERIALS AND METHODS

Geologic and geomorphic setting

Bedrock in the Naqsaq and Ayr Lake valleys consists of Archean monzogranite, granodiorite, tonalite gneiss, and Proterozoic banded migmatite (*42*). During the Last Glacial Maximum, alpine glaciers in Clyde Inlet and Ayr Lake valley merged with major Laurentide Ice Sheet outlet glaciers (Fig. 1; main text) (*21*, *43*). Regional deglaciation was under way by ~14.7 ka, with local deglaciation of the Ayr Lake valley occurring by ~13.7 ka based on numerous ^{10}Be ages (*21*), and deglaciation of Naqsaq valley occurred sometime before ~9.4 cal ka B.P. (thousand calibrated years before the present) based on a minimum constraining radiocarbon age (*44*). Presently, these valleys host small alpine glaciers extending from high-elevation cold-based to polythermal ice caps. Moraine mapping in Naqsaq valley shown in Fig. 2 was conducted in the field and on aerial photographs. The Naqsaq moraine system is dominated by a fresh and steep moraine with minor recessional ridges, and just beyond the fresh moraine is a series of nested right-lateral moraine segments displaying slightly more subdued morphologies (Fig. 2; main text). This moraine sequence comprises six individual moraines, and we dated five of these moraines with cosmogenic ^{10}Be (Fig. 2 and fig. S4); only a small portion of the outermost moraine is preserved, and there were no boulders suitable for ^{10}Be dating resting on this moraine crest. However, this undated moraine must be older than the age of M1 (1040 ± 60 CE). In Ayr Lake valley, the fresh and steep moraine is fronted by a series of right-lateral moraine segments. Because of the lack of suitable boulders in this moraine sequence, we were only able to sample four boulders on the outermost moraine.

In western Greenland, the crystalline bedrock primarily consists of Precambrian granodioritic and tonalitic gneisses (*45*). Local alpine glaciers on the Nuussuaq Peninsula likely coalesced the Greenland Ice Sheet during the Last Glacial Maximum, and the most direct limits on the timing of local deglaciation are minimum constraining radiocarbon ages of ~11.8 and 10.0 cal ka B.P. from western and eastern Nuussuaq, respectively (*46*, *47*). These ages are supported by numerous radiocarbon and ^{10}Be ages that constrain deglaciation of the Disko Bugt region immediately to the south of Nuussuaq to ~11 to 10 ka [reviewed by Kelley *et al.* (*48*) and references therein]. We focused on a moraine sequence in the Uigordleq Lake valley in eastern Nuussuaq (fig. S1). The moraines were deposited by an outlet glacier of an unnamed local ice cap, independent of the Greenland Ice Sheet that flows into the Uigordleq sarqâ; during the maximum late Holocene ice extent, the glacier terminated and calved into Uigordleq Lake. We mapped the well-preserved right-lateral moraines into two assemblages based on vegetative cover and geomorphic position; the "inner" moraines are steep, fresh, unvegetated, and presently ice-cored, whereas the "outer" moraines are more subdued and more heavily lichen-covered. The inner moraines consist of at least four recessional right-lateral ridges. The outer moraines have low relief and rest directly outside of the inner moraines (fig. S1). We targeted the outer right-lateral moraine complex for ^{10}Be dating. It consists of five subdued moraine ridges which we clustered into three moraine groups: proximal, intermediate, and distal. The proximal and intermediate moraines are single moraine crests; the outermost moraine set is composed of three small moraine ridges. Differences in relief between the moraine crests are small (~2 to 3 m). The outermost two moraines are hummocky and have relatively more subdued morphologies than the proximal moraine. To minimize outliers associated with reworking (for example, boulder rotation), we targeted samples from large, stable boulders located on prominent ridges within the moraine complex (fig. S5).

Geochemistry and accelerator mass spectrometry

Samples from Baffin Island were processed at the Lamont-Doherty Earth Observatory (LDEO) cosmogenic dating laboratory, and

samples from Greenland were processed at the University at Buffalo Cosmogenic Isotope Laboratory following well-established protocols; standard quartz isolation and beryllium extraction techniques [for example, Schaefer *et al.* (*49*)] were applied in both laboratories (www.ldeo.columbia.edu/res/pi/tcn/LDEO_Cosmogenic_Nuclide_Lab/Chemistry.html). Accelerator mass spectrometric analysis for all samples was completed at the Center for Accelerator Mass Spectrometry at Lawrence Livermore National Laboratory. All samples were measured relative to the 07KNSTD standard with a $^{10}Be/^{9}Be$ ratio of 2.85×10^{-12} (*50*).

For Baffin Island samples, the 1σ analytical error ranged from 2.7 to 10.8%, with an average of 4.7% (table S1). These uncertainties are slightly higher than the typical uncertainties for LDEO processed samples (~2%), but these higher uncertainties are expected because of the low ^{10}Be concentrations being measured—a function of the sample age and low sample elevation (table S1). ^{10}Be concentrations ranged from ~5000 to 6000 ^{10}Be atoms g^{-1} for the oldest moraine, down to as low as ~1260 ^{10}Be atoms g^{-1} for the youngest moraine (M5). The overall batch-specific blank corrections ranged from ~1 to 4% for most samples, but for the youngest samples (M5 crest), the blank correction ranged from ~5 to 11% (table S1).

For the western Greenland samples, the 1σ analytical error ranged from 3.6 to 13.1%, with an average of 7.7%. Sample ^{10}Be concentrations ranged from ~5000 to 8200 ^{10}Be atoms g^{-1}, and the overall batch-specific blank corrections ranged from ~3.5 to 28.4%, with an average of 14.1% (tables S1 and S2).

^{10}Be production rate, ^{10}Be age calculations, and ^{10}Be assumptions

The location and elevation of each sample were recorded with a handheld GPS (Global Positioning System) receiver with a vertical uncertainty of ~10 m, equating to a <1% uncertainty in ^{10}Be age. In Baffin Island, the GPS receiver was calibrated each morning at a known elevation (sea level). All samples were collected from the uppermost horizontal or near horizontal boulder surfaces using a hammer and chisel, a handheld rotary saw with a diamond-bit blade, or some combination of the two. A clinometer was used to measure sample-specific shielding by the surrounding topography. All sampled boulders were resting directly on their respective moraine crests.

All ^{10}Be ages were calculated with the locally constrained Baffin Bay ^{10}Be production rate (3.96 ± 0.07 atoms g^{-1} a^{-1}) (*26*) and time-variant "Lm" scaling (*51*, *52*). Ages were calculated using a slightly modified version of the Matlab code developed for the CRONUS-Earth online ^{10}Be exposure age calculator (*53*). Calendar ages of each moraine reported in the main text and those reported in figs. S2 and S3 were calculated by subtracting the moraine ^{10}Be exposure age from the year of sample collection (2013 CE). The production rate uncertainty has been propagated through in the quadrature for the stated moraine ages.

We use "Lm" scaling, but because of our sample sites' high latitude (~70°N), the effects of fluctuations in the geomagnetic field on ^{10}Be production are minimal, and hence, all scaling schemes yield similar ages (table S3). Moreover, the reference ^{10}Be production rate for "Lm" scaling is identical to the reference ^{10}Be production rate for "St" scaling (constant ^{10}Be production) because of the similar settings of each production rate calibration site (high latitude and low elevation), thus highlighting the negligible influence of the geomagnetic field on ^{10}Be production at these high latitudes. Although all scaling schemes result in similar ^{10}Be ages at our study sites (within ~2%), the neutron monitor-based schemes (De, Du, Li; table S2) (*54*–*56*) likely overestimate the altitude dependence of ^{10}Be production (*57*, *58*), and therefore, we do not consider them further. We also note that because the Baffin Bay production rate calibration data set comprises data sets that are ~8200 and 9200 years, minor fluctuations in the strength of the magnetic field are likely offset. We lose this advantage of integrating millennial-scale changes in the magnetic field over the short exposure durations during the late Holocene presented here, where changes in magnetic field strength may be the most pronounced (*27*). Unfortunately, there is not a ^{10}Be production rate calibration that only spans the last ~1000 years, so it remains difficult to evaluate any effect these changes would have on very young ^{10}Be ages. However, the Baffin Bay ^{10}Be calibration data are the youngest calibration data available, so the resulting uncertainty is likely less than if a significantly older ^{10}Be calibration data set is used. Nonetheless, the effects of late Holocene geomagnetic fluctuations are likely minimized at our sites' high latitude and associated low effective vertical cutoff rigidity values.

The crystalline boulder lithologies in Naqsaq, Ayr Lake, and Uigordleq Lake valleys are resistant to erosion and commonly displayed glacial striations, indicating that there has been negligible, if any, surface erosion since initial boulder exposure. Moreover, erosion is likely to be minimal on the time scales considered here (~1000 years and younger), and we do not consider the effects of erosion when calculating ^{10}Be ages. We did not sample boulder areas that had any obvious signs of surface spallation. In addition, we do not apply a correction for potential snow cover. Accounting for an average yearly snow depth of ~195 cm (average yearly snowfall at Clyde River from 1981 to 2010; source: Environment Canada) and snow density of 0.2 g cm^{-3} (*59*) would result in ^{10}Be ages that are ~7% older, but this assumes that all snow remains on the boulder's surface (no melt or wind). We think that this is highly unlikely because all boulders sampled for this study were collected from windswept moraine crests. Thus, we consider such a snow-shielding correction to be a significant overestimate. Furthermore, on Baffin Island, we conducted fieldwork during the time of maximum snow cover (spring) and observed no significant snow accumulation on moraine ridges; snow had only accumulated in the protected swales between moraine ridges. We also made no correction for isostatic rebound. Although both field areas have undergone isostatic uplift since regional deglaciation, local and regional uplift curves reveal that almost all uplift occurred shortly after regional deglaciation in the early to middle Holocene (*44*, *60*), and hence, negligible uplift has occurred over the last ~1000 years, the maximum age of our samples presented here.

Geological processes could also potentially influence our moraine ages. Moraine degradation can result in anomalously young ^{10}Be ages [for example, Briner *et al.* (*61*) and Putkonen and Swanson (*62*)], and furthermore, efforts have been made to statistically model the "true" age of a moraine based on a given ^{10}Be age population and a numerical representation of geological processes such as moraine degradation (*63*). Here, moraine degradation via melt-out of an internal ice core could result in anomalously young ^{10}Be ages for our ice-cored moraines. However, ^{10}Be ages presented here are internally consistent on each moraine crest, and we do not observe a young tail on the ^{10}Be age distribution that would be evident if moraine degradation were significantly affecting our ^{10}Be age population as has been demonstrated by previous authors (*61*, *62*). One possibility is that there has not been significant melt-out (degradation) of our sampled ice-cored moraines, or melt-out has occurred in a relatively uniform fashion and our

boulders resting on the moraine crest have been unaffected by the melt-out process. Although the latter seems unlikely, the internal consistency of our ^{10}Be age populations and the lack of anomalously young outliers suggest that our ^{10}Be ages are not significantly influenced, if at all, by moraine degradation.

We acknowledge that some scatter exists in the ^{10}Be ages in Uigordleq Lake valley chronology (fig. S1 and table S1). However, the proximal moraine crest is firmly dated to 1130 ± 40 CE (n = 3), with all ^{10}Be ages in close agreement, and serves as a natural pinning point for the overall chronology. On the basis of the age of the proximal moraine and classic laws of morphostratigraphy, the outer two moraines must have been deposited before 1130 ± 40 CE. If no outliers are removed and ^{10}Be ages are averaged per moraine, then the intermediate moraine age is 790 ± 270 CE and the distal moraine age is 910 ± 190 CE. The average ages of the two outer moraines overlap within uncertainty and are indistinguishable from each other; both are older than the proximal moraine, thus within morphostratigraphical order. In addition, given their overlapping uncertainties, it is likely that these moraines were deposited in close succession. We cannot rule out the possibility of isotopic inheritance, potentially via boulder reworking, or postdeposition boulder exhumation, which may explain the higher degree of scatter on the intermediate and distal moraine crests. However, because it is difficult to identify outliers based on statistical procedures, we opt for the more conservative treatment of averaging all ^{10}Be ages per moraine group. Nonetheless, we can confidently conclude that the intermediate and distal moraines must have been deposited sometime in the late Holocene before 1130 ± 40 CE.

SUPPLEMENTARY MATERIALS

Supplementary material for this article is available at http://advances.sciencemag.org/cgi/content/full/1/11/e1500806/DC1

Fig. S1. Uigordleq Lake valley moraine complex and ^{10}Be ages.

Fig. S2. Normal kernel density estimates of ^{10}Be ages grouped by moraine from Baffin Island.

Fig. S3. Comparison of moraine ages between Naqsaq, Ayr, and Uigordleq Lake valley moraines.

Fig. S4. Representative moraine boulders from Naqsaq valley.

Fig. S5. Representative moraine boulders from Uigordleq Lake valley.

Table S1. ^{10}Be sample input information.

Table S2. Process blank ^{10}Be data.

Table S3. ^{10}Be ages using alternative scaling schemes.

REFERENCES AND NOTES

1. H. H. Lamb, The early medieval warm epoch and its sequel. *Palaeogeogr. Palaeoclimatol. Palaeoecol.* **1**, 13–37 (1965).
2. J. M. Grove, *The Little Ice Age* (Methuen, New York, 1988).
3. G. Bond, B. Kromer, J. Beer, R. Muscheler, M. N. Evans, W. Showers, S. Hoffmann, R. Lotti-Bond, I. Hajdas, G. Bonani, Persistent solar influence on North Atlantic climate during the Holocene. *Science* **294**, 2130–2136 (2001).
4. D. C. Lund, J. Lynch-Stieglitz, W. B. Curry, Gulf Stream density structure and transport during the past millennium. *Nature* **444**, 601–604 (2006).
5. G. H. Miller, Á. Geirsdóttir, Y. Zhong, D. J. Larsen, B. L. Otto-Bliesner, M. M. Holland, D. A. Bailey, K. A. Refsnider, S. J. Lehman, J. R. Southon, C. Anderson, H. Björnsson, T. Thordarson, Abrupt onset of the Little Ice Age triggered by volcanism and sustained by sea-ice/ocean feedbacks. *Geophys. Res. Lett.* **39**, L02708 (2012).
6. V. Trouet, J. Esper, N. E. Graham, A. Baker, J. D. Scourse, D. C. Frank, Persistent positive North Atlantic Oscillation mode dominated the medieval climate anomaly. *Science* **324**, 78–80 (2009).
7. M. E. Mann, Z. Zhang, S. Rutherford, R. S. Bradley, M. K. Hughes, D. Shindell, C. Ammann, G. Faluvegi, F. Ni, Global signatures and dynamical origins of the Little Ice Age and medieval climate anomaly. *Science* **326**, 1256–1260 (2009).
8. D. Bruun, *The Icelandic Colonization of Greenland and the Finding of Vineland* (Meddelelser om Grønland, Museum Tusculanum Press, Copenhagen, 1918), vol. 57, pp. 1–228.
9. W. Dansgaard, S. J. Johnsen, N. Reeh, N. Gundestrup, H. B. Clausen, C. U. Hammer, Climatic changes, Norseman and modern man. *Nature* **255**, 24–28 (1975).
10. M. Magnússon, H. Pálsson, *The Vinland Sagas: The Norse Discovery of America: "Grælendinga Saga" and "Eirik's Saga"* (Penguin Book, London, 1965).
11. A. S. Ingstad, *The Discovery of a Norse Settlement in America, Vol. 1* (Universitetsforlaget, Oslo, 1977).
12. P. D. Sutherland, P. H. Thompson, P. A. Hunt, Evidence of early metalworking in Arctic Canada. *Geoarcheology* **30**, 74–78 (2015).
13. H. Pringle, "Evidence of Viking outpost found in Canada", *National Geographic News*, 19 October 2012.
14. L. K. Barlow, J. P. Sadler, A. E. J. Ogilvie, P. C. Buckland, T. Amorosi, J. H. Ingimundarson, P. Skidmore, A. J. Dugmore, T. H. McGovern, Interdisciplinary investigations of the end of the Norse Western Settlement in Greenland. *Holocene* **7**, 489–499 (1977).
15. W. P. Patterson, K. A. Dietrich, C. Holmden, J. T. Andrews, Two millennia of North Atlantic seasonality and implications for Norse colonies. *Proc. Natl. Acad. Sci. U.S.A.* **107**, 5306–5310 (2012).
16. A. J. Dugmore, T. H. McGovern, O. Vésteinsson, J. Arneborg, R. Streeter, C. Keller, Cultural adaptation, compounding vulnerabilities and conjunctures in Norse Greenland. *Proc. Natl. Acad. Sci. U.S.A.* **109**, 3658–3663 (2012).
17. J. Arneborg, N. Lynnerup, J. Heinemeier, Human diet and subsistence patterns in Norse Greenland AD c.980–AD c.1450: Archaeological interpretations. *J. North Atlantic* **3**, 119–133 (2012).
18. J. Oerlemans, Extracting a climate signal from 169 glacier records. *Science* **308**, 675–677 (2005).
19. H. Holzhauser, M. Magny, H. J. Zumbuuhl, Glacier and lake-level variations in west-central Europe over the last 3500 years. *Holocene* **15**, 789–801 (2005).
20. J. M. Licciardi, J. M. Schaefer, J. R. Taggart, D. C. Lund, Holocene glacier fluctuations in the Peruvian Andes indicate northern climate linkages. *Science* **325**, 1677–1679 (2009).
21. N. E. Young, J. P. Briner, D. H. Rood, R. C. Finkel, Glacier extent during the Younger Dryas and 8.2-ka event on Baffin Island, Arctic Canada. *Science* **337**, 1330–1333 (2012).
22. J. S. Stroup, M. A. Kelly, T. V. Lowell, P. J. Applegate, J. A. Howley, Late Holocene fluctuations of Qori Kalis outlet glacier, Quelccaya Ice Cap, Peruvian Andes. *Geology* **42**, 347–350 (2014).
23. S. C. Porter, Neoglaciation in the American Cordilleras, in *Encyclopedia of Quaternary Science*, S. Elias, Ed. (Elsevier, Amsterdam, 2007), pp. 1133–1142.
24. P. T. Davis, Neoglacial moraines on Baffin Island, in *Quaternary Environments: Eastern Canadian Arctic, Baffin Bay and Western Greenland*, J. T. Andrews, Ed. (Allen and Unwin, London, 1985), pp. 682–718.
25. G. Osborn, D. McCarthy, A. LaBrie, R. Burke, Lichenometric dating: Science or pseudo-science. *Quat. Res.* **83**, 1–12 (2015).
26. N. E. Young, J. M. Schaefer, J. P. Briner, B. M. Goehring, A ^{10}Be production-rate calibration for the Arctic. *J. Quat. Sci.* **28**, 515–526 (2013).
27. F. M. Phillips, D. C. Argento, G. Balco, M. W. Caffee, J. Clem, T. J. Dunai, R. Finkel, B. Goehring, J. C. Gosse, A. M. Hudson, A. J. T. Jull, M. A. Kelly, M. Kurz, D. Lal, N. Lifton, S. M. Marrero, K. Nishiizumi, R. C. Reedy, J. Schaefer, J. O. H. Stone, T. Swanson, M. G. Zreda, The CRONUS-Earth Project: A synthesis. *Quat. Geochronol.*, 10.1016/ j.quageo.2015.09.006 (2015).
28. G. Balco, Contributions and unrealized potential contributions of cosmogenic-nuclide exposure dating to glacier chronology, 1990–2010. *Quat. Sci. Rev.* **30**, 3–27 (2011).
29. A. E. Putnam, J. M. Schaefer, G. H. Denton, D. J. A. Barrell, R. C. Finkel, B. G. Andersen, R. Schwartz, T. J. H. Chinn, A. M. Doughty, Regional climate control of glaciers in New Zealand and Europe during the pre-industrial Holocene. *Nat. Geosci.* **5**, 627–630 (2012).
30. I. Schimmelpfennig, J. M. Schaefer, N. Akçar, T. Koffman, S. Ivy-Ochs, R. Schwartz, R. C. Finkel, S. Zimmerman, C. Schlüchter, A chronology of Holocene and Little Ice Age glacier culminations of the Steingletscher, central Alps, Switzerland, based on high-sensitivity beryllium-10 moraine dating. *Earth Planet. Sci. Lett.* **393**, 220–230 (2014).
31. A. B. Gibbons, J. D. Megeath, K. P. Pierce, Probability of moraine survival in a succession of glacier advances. *Geology* **12**, 327–330 (1984).
32. B. Pratt-Sitaula, D. W. Burbank, A. M. Heimsath, N. F. Humphrey, M. Oskin, J. Putkonen, Topographic control of asynchronous glacial advances: A case study from Annapurna, Nepal, *Geophys. Res. Lett.* **38**, L24502 (2011).
33. R. M. Koerner, Mass balance of glaciers in the Queen Elizabeth Islands, Nunavut, Canada. *J. Glaciol.* **42**, 417–423 (2005).
34. R. B. Alley, *GISP2 Ice Core Temperature and Accumulation Data. IGBP PAGES/World Data Center for Paleoclimatology Data Contribution Series #2004-013* (NOAA/NGDC Paleoclimatology Program, Boulder, CO, 2004).

35. M.-A. Sicre, K. Weckström, M.-S. Seidenkrantz, A. Kuijpers, M. Benetti, G. Masse, U. Ezat, S. Schmidt, I. Bouloubassi, J. Olsen, M. Khodri, J. Mignot, Labrador current variability over the last 2000 years. *Earth Planet. Sci. Lett.* **400**, 26–32 (2014).
36. M.-S. Seidenkrantz, L. Roncaglia, A. Fischel, C. Heilmann-Clausen, A. Kuijpers, M. Moros, Variable North Atlantic climate seesaw patterns documented by a late Holocene marine record from Disko Bugt, West Greenland. *Mar. Micropaleontol.* **68**, 66–83 (2008).
37. T. Kobashi, K. Kawamura, J. P. Severinghaus, J.-M. Barnola, T. Nakaegawa, B. M. Vinther, S. J. Johnsen, J. E. Box, High variability of Greenland surface temperature over the past 4000 years estimated from trapped air in an ice core. *Geophys. Res. Lett.* **38**, L21501 (2011).
38. W. J. D'Andrea, Y. Huang, S. C. Fritz, N. John Anderson, Abrupt Holocene climate change as an important factor for human migration in West Greenland. *Proc. Natl. Acad. Sci. U.S.A.* **108**, 9765–9769 (2011).
39. G. Massé, S. J. Rowland, M.-A. Sicre, J. Jacob, E. Jansen, S. T. Belt, Abrupt climate changes for Iceland during the last millennium: Evidence from high resolution sea ice reconstructions. *Earth Planet. Sci. Lett.* **269**, 565–569 (2008).
40. D. J. Larsen, G. H. Miller, Á. Geirsdóttir, T. Thordarson, A 3000-year varved record of glacier activity and climate change from the proglacial lake Hvítárvatn, Iceland. *Quat. Sci. Rev.* **30**, 2715–2731 (2011).
41. J. E. Box, Survey of Greenland instrumental temperature records: 1873–2001. *Int. J. Climatol.* **22**, 1829–1847 (2002).
42. G. D. Jackson, S. L. Blusson, W. J. Crawford, A. Davidson, W. C. Morgan, E. H. Kranck, G. Riley, K. E. Eade, Geology, Clyde River, District of Franklin: Geological Survey of Canada, "A" Series Map 1582A, scale 1:250,000 (1984).
43. J. P. Briner, G. H. Miller, P. Thompson Davis, R. C. Finkel, Cosmogenic radionuclides form fiord landscapes support differential erosion by overriding ice sheets. *Geol. Soc. Am. Bull.* **118**, 406–420 (2006).
44. J. P. Briner, I. Overeem, G. Miller, R. Finkel, The deglaciation of Clyde Inlet, northeastern Baffin Island, Arctic Canada, *J. Quat. Sci.* **22**, 223–232 (2007).
45. J. A. Chalmers, T. C. R. Pulvertaft, C. Marcussen, A. K. Pedersen, New insights into the structure of the Nuussuaq Basin, central West Greenland. *Mar. Petrol. Geol.* **16**, 197–224 (1999).
46. A. Weidick, *Observations on Some Holocene Glacier Fluctuations in West Greenland* (Meddelelser om Grønland, C. A. Reitzel, Copenhagen, 1968), vol. 165, pp. 1–202.
47. O. Bennike, Palaeoecological studies of Holocene lake sediments from West Greenland. *Palaeogeogr. Palaeoclimatol. Palaeoecol.* **155**, 285–304 (2000).
48. S. E. Kelley, J. P. Briner, N. E. Young, Rapid ice retreat in Disko Bugt supported by ^{10}Be dating of the last recession of the western Greenland Ice Sheet. *Quat. Sci. Rev.* **82**, 13–22 (2013).
49. J. M. Schaefer, G. H. Denton, M. Kaplan, A. Putnam, R. C. Finkel, D. J. A. Barrell, B. G. Andersen, R. Schwartz, A. Mackintosh, T. Chinn, C. Schlüchter, High-frequency Holocene glacier fluctuations in New Zealand differ from the northern signature. *Science* **324**, 622–625 (2009).
50. K. Nishiizumi, M. Imamura, M. W. Caffee, J. R. Southon, R. C. Finkel, J. McAninch, Absolute calibration of ^{10}Be AMS standards. *Nucl. Instrum. Meth. B* **258**, 403–413 (2007).
51. D. Lal, Cosmic ray labeling of erosion surfaces: In situ nuclide production rates and erosion models, *Earth Planet. Sci. Lett.* **104**, 424–439 (1991).
52. J. Stone, Air pressure and cosmogenic isotope production. *J. Geophys. Res.* **105**, 23753–23759 (2000).
53. G. Balco, J. O. Stone, N. A. Lifton, T. J. Dunai, A complete and easily accessible means of calculating surface exposure ages or erosion rates from ^{10}Be and ^{26}Al measurements. *Quat. Geochronol.* **3**, 174–195 (2008).
54. D. Desilets, M. Zreda, Spatial and temporal distribution of secondary cosmic-ray nucleon intensities and applications to in situ cosmogenic dating. *Earth Planet. Sci. Lett.* **206**, 21–42 (2003).
55. J. T. Dunai, Scaling factors for production rates of in situ produced cosmogenic nuclides: A critical reevaluation. *Earth Planet. Sci. Lett.* **176**, 157–169 (2000).
56. N. A. Lifton, J. W. Bieber, J. M. Clem, M. L. Duldig, P. Evenson, J. E. Humble, R. Pyle, Addressing solar modulation and long-term uncertainties in scaling secondary cosmic rays for in situ cosmogenic nuclide applications. *Earth Planet. Sci. Lett.* **239**, 140–161 (2005).
57. N. A. Lifton, T. Sato, T. J. Dunai, Scaling in situ cosmogenic nuclide production rates using analytical approximations to atmospheric cosmic-ray fluxes. *Earth Planet. Sci. Lett.* **386**, 149–160 (2014).
58. B. Borchers, S. Marrero, G. Balco, M. Caffee, B. Goehring, N. Lifton, K. Nishiizumi, F. Phillips, J. Schaefer, J. Stone, Geological calibration of spallation production rates in the CRONUS-Earth project. *Quat. Geochronol.*, 10.1016/j.quageo.2015.01.009 (2015).
59. J. C. Gosse, F. M. Phillips, Terrestrial in situ cosmogenic nuclides: Theory and application. *Quat. Sci. Rev.* **20**, 1475–1560 (2001).
60. A. J. Long, S. A. Woodroffe, D. H. Roberts, S. Dawson, Isolation basins, sea-level changes and the Holocene history of the Greenland Ice Sheet. *Quat. Sci. Rev.* **30**, 3748–3768 (2011).
61. J. P. Briner, D. S. Kaufman, W. F. Manley, R. C. Finkel, M. W. Caffee, Cosmogenic exposure dating of late Pleistocene moraine stabilization in Alaska. *GSA Bull.* **117**, 1108–1120 (2005).
62. J. Putkonen, T. Swanson, Accuracy of cosmogenic ages for moraines. *Quat. Res.* **59**, 255–261 (2003).
63. P. J. Applegate, N. M. Urban, K. Keller, T. V. Lowell, B. J. C. Laabs, M. A. Kelly, R. B. Alley, Improved moraine age interpretations through explicit matching of geomorphic process models to cosmogenic nuclide measurements from single landforms. *Quat. Res.* **77**, 293–304 (2012).
64. A. Margreth, A. S. Dyke, J. C. Gosse, A. M. Telka, Neoglacial ice expansion and late Holocene cold-based ice cap dynamics on Cumberland Peninsula, Baffin Island, Arctic Canada. *Quat. Sci. Rev.* **91**, 242–256 (2014).

Acknowledgments: We thank the Nunavut Research Institute and the Inuit of Clyde River for assistance and access to the Baffin Island field sites. We also thank S. Cronauer for help with sample preparation, and B. Finkel and S. Zimmerman for careful ^{10}Be measurements at Lawrence Livermore National Laboratory's Center for Accelerator Mass Spectrometry. **Funding:** N.E.Y. acknowledges support from a Lamont-Doherty Postdoctoral Fellowship, the Lamont Climate Center, and the Comer Science and Educational Foundation. Partial support was provided by NSF award #1417675 to N.E.Y. and J.M.S. **Author contributions:** N.E.Y., J.M.S., and J.P.B. initiated this research. N.E.Y., A.D.S., and J.P.B. conducted fieldwork. N.E.Y. and A.D.S. completed the chemical analyses. N.E.Y. wrote the paper, with all authors contributing toward interpreting the results and refining the paper. **Competing interests:** The authors declare that they have no competing interests. **Data and materials availability:** All of the raw data can be found in the accompanying supplementary material. This is LDEO contribution 7950.

Submitted 19 June 2015
Accepted 23 October 2015
Published 4 December 2015
10.1126/sciadv.1500806

Citation: N. E. Young, A. D. Schweinsberg, J. P. Briner, J. M. Schaefer, Glacier maxima in Baffin Bay during the Medieval Warm Period coeval with Norse settlement. *Sci. Adv.* **1**, e1500806 (2015).